

Evolution of the Fermi surface across the metamagnetic transition in $\text{Sr}_4\text{Ru}_3\text{O}_{10}$

Y. J. Jo¹, L. Balicas¹, N. Kikugawa², K. Storr³, M. Zhou⁴, and Z. Q. Mao⁴

¹*National High Magnetic Field Laboratory, Florida State University, Tallahassee-FL 32306, USA*

²*School of Physics and Astronomy, University of St. Andrews, St. Andrews, Fife KY16 9SS, UK*

³*Department of Physics, Prairie View A&M University, Texas 77446-0519, USA* and

⁴*Department of Physics, Tulane University, New Orleans, Louisiana 70118, USA*

(Dated: October 24, 2019)

We report an electrical transport study in high quality single crystals of $\text{Sr}_4\text{Ru}_3\text{O}_{10}$ at very high magnetic fields and low temperatures and in its ferromagnetic state. For fields aligned a few degrees away from the inter-plane direction we observe Shubnikov-de Haas oscillations showing a non-trivial evolution of the geometry of the Fermi surface across an anisotropic metamagnetic transition. Our observations suggest either that localized and itinerant bands coexist in this system, the former leading to the ferromagnetic response and the later to itinerant metamagnetic behavior, or that itinerant metamagnetism emerges from a Stoner-like ferromagnetic ground state.

PACS numbers: 71.18.+y, 72.15.Gd, 75.30.-m

Metamagnetism is usually understood as a rapid increase of the magnetization of a given system in a narrow range of magnetic fields. In a spin localized picture, it would correspond to the field-induced suppression of, for instance, antiferromagnetic order via a spin-flop and/or a subsequent spin-flip transition [1]. While in itinerant systems, metamagnetism is explained in terms of the field-induced spin-polarization of the Fermi surface and concomitant field-tuned proximity of the Fermi level to a van-Hove singularity [2].

The ruthenates, $\text{Sr}_3\text{Ru}_2\text{O}_7$ in particular, were reported to display complex metamagnetic behavior, including the possibility of quantum-criticality by tuning to zero temperature the end point of a first-order metamagnetic transition [3] which seems to lead, in high purity samples, to the formation of a new phase at low temperatures [4]. While in the Ca rich metallic region of the $\text{Ca}_{2-x}\text{Sr}_x\text{RuO}_4$ series, metamagnetism is followed by a remarkable magnetoelastic coupling [5] resulting perhaps from the field-induced suppression or reconfiguration of an orbital-ordered state [6]. Complex and highly anisotropic metamagnetic behavior has also been recently reported in the tri-layered $\text{Sr}_4\text{Ru}_3\text{O}_{10}$ compound [8] which is a structurally distorted ferromagnet: the RuO_6 octahedra in the outer two layers of each triple layer are rotated by an average of 5.6° around the c-axis, while the octahedra of the inner layers are rotated in the opposite sense by an average of 11.0° [7]. It displays a Curie temperature $T_c \sim 100$ K (see Fig. 1) and a saturated moment of $\sim 1\mu_B$ per Ru^{4+} ion, which according to the strong magnetoelastic coupling observed by Raman spectroscopy is probably *localized* in the Ru site [9] and directed essentially along the c-axis [7, 8]. This ferromagnetic (FM) transition is followed by an additional broad peak in the magnetic susceptibility at $T_M \simeq 50$ K in flux grown samples [7, 8], $T_M \simeq 75$ K in floating zone grown crystals, which is claimed to result from the “locking” of the moments into a canted antiferromagnetic configura-

tion [9]. However, neutron experiments do not reveal any evidence of antiferromagnetism below 50K [10].

In the $\text{Ca}_{2-x}\text{Sr}_x\text{RuO}_4$ system as Sr is replaced by Ca the rotation of the RuO_6 octahedra leads to the renormalization of the bandwidth of the γ band resulting from the d_{xy} planar orbitals [11] triggering a nearly ferromagnetic response [11, 12]. Furthermore, this rotation has also been claimed to lead to the localization of the γ band [13]. Thus it is not surprising to observe ferromagnetism and evidence for localization in $\text{Sr}_4\text{Ru}_3\text{O}_{10}$. In fact, one needs a field of the order of only a few hundred Gauss, applied along the c-axis, to polarize the moments to a value $S \geq 1/2$ [7, 8]. The placement of four carriers on the three Ru $4d_{t_{2g}}$ orbitals should lead, according to Hund’s rule and in a spin-localized picture, to $S = 1$. A value $S = 1/2$ in the Ca rich metallic region of the $\text{Ca}_{2-x}\text{Sr}_x\text{RuO}_4$ series was explained in terms of an orbital-ordered state triggered by an orbital selective Mott transition [14].

In $\text{Sr}_4\text{Ru}_3\text{O}_{10}$ when a magnetic field is applied along an in-plane direction at low temperatures, it exhibits a sharp and hysteretic metamagnetic transition at a critical field $H_{MM} \simeq 2$ T [7, 8]. In high quality single crystals the observed hysteresis exhibits ultra sharp steps in the resistivity claimed to result from domain formation and possible electronic phase separation [15]. As the field is tilted away from an in-plane direction the transition broadens considerably and moves towards higher fields while the hysteresis virtually disappears [8]. This is particularly remarkable since this metamagnetic behavior occurs under a sizeable component of the external field applied along the inter-plane direction, i.e., when the moments are expected to be completely polarized along the c-axis.

Here, in order to understand the origin of the metamagnetic behavior of $\text{Sr}_4\text{Ru}_3\text{O}_{10}$, we performed electrical transport measurements at very high magnetic fields and low temperatures in two batches of single crystals, one having a residual resistivity $\rho_0 \simeq 6\mu\Omega\text{cm}$, where

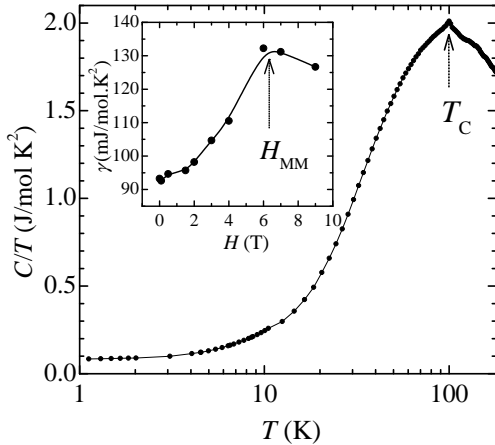


FIG. 1: Heat capacity C normalized by temperature T of a $\text{Sr}_4\text{Ru}_3\text{O}_{10}$ single crystal as a function of temperature T . Only one small anomaly is observed around $T_c \sim 100$ K. Inset: The Sommerfeld coefficient or the electronic contribution to the heat capacity as a function of the field H applied nearly parallel to the in-plane direction and as one crosses a metamagnetic transition.

we performed inter-plane transport measurements, and a second one displaying a ρ_0 between 1.5 and 2 $\mu\Omega\text{cm}$ which was used mainly for in-plane transport studies. Our goal is to explore the possibility that the metamagnetism within the spin-polarized state might involve the bands that remain itinerant by measuring the evolution of the geometry of the Fermi surface across the transition via the Shubnikov-de-Haas effect. Since, as discussed in Ref. [2], the behavior of the magnetic susceptibility, displaying a ferromagnetic transition and a broad maximum as the temperature is decreased, could be understood in terms of the evolution of the entropy of an itinerant system very close to a van Hove singularity, i.e., without invoking spin-canting, which is consistent with neutron experiments [10] and suggests the possibility of itinerant metamagnetism.

Our crystals were grown by a floating-zone (FZ) technique [16]. Crystals selected for the measurements were well characterized by x-ray diffraction and were found to be pure $\text{Sr}_4\text{Ru}_3\text{O}_{10}$. Conventional four-probe techniques were used in conjunction with a single axis-rotator inserted in a ^3He cryostat. High magnetic fields up to 45 T were provided by the hybrid magnet at the NHMFL.

Figure 1 displays the heat capacity C normalized by the temperature T and as a function T for a $\text{Sr}_4\text{Ru}_3\text{O}_{10}$ single crystal in absence of an external field. A weak anomaly is seen at $T_c \simeq 100$ K indicating the onset of ferromagnetism. No anomaly is seen below T_c that one could associate with the proposed spin canting transition [9]. The electronic contribution to C/T , the so-called Sommerfeld coefficient γ is $\simeq 92.5$ mJ/molK 2 or ~ 30 mJ/Ru-molK 2 and is comparable with what is ob-

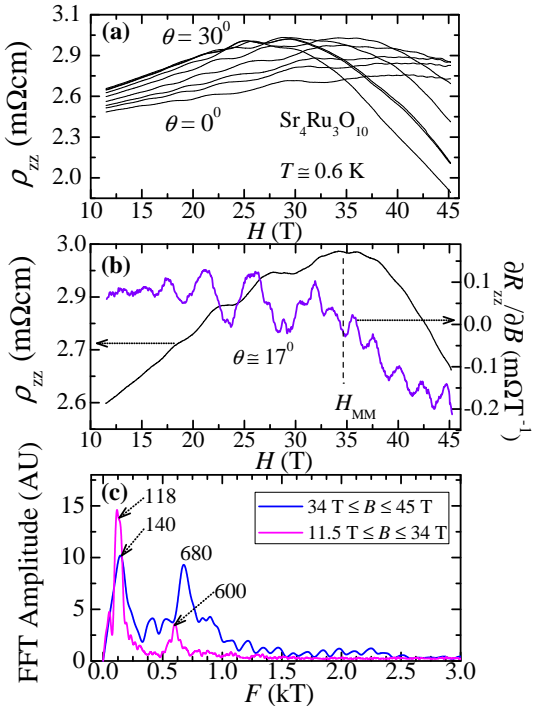


FIG. 2: (a) The inter-plane resistivity ρ_{zz} for a $\text{Sr}_4\text{Ru}_3\text{O}_{10}$ single crystal as a function of magnetic field H at $T \simeq 0.5$ K and for several angles θ between H and the inter-plane c-axis. Notice both the presence of Shubnikov de Haas oscillations and the rapid decrease in ρ_{zz} when the metamagnetic transition is crossed at higher angles. (b) ρ_{zz} and its derivative $\partial\rho_{zz}/\partial H$ as a function B at $T \simeq 0.5$ K and for $\theta = 17 \pm 2^\circ$. Notice how the Shubnikov de Haas oscillatory pattern changes at the transition. (c) The FFT spectrum of the oscillatory component of ρ_{zz} for fields above and below 34 T. Notice how the observed peaks are displaced towards higher frequencies above the transition.

tained in Sr_2RuO_4 [17]. Since the density of states at the Fermi level has a similar value in both systems and since Sr_2RuO_4 is a Pauli paramagnet, it seems difficult to conciliate this observation with a Stoner-like itinerant-ferromagnetic scenario for $\text{Sr}_4\text{Ru}_3\text{O}_{10}$. Coupled to the Curie-Weiss type of susceptibility seen above 180K (not shown here), which yields an effective moment of 1.15 μ_B , this suggests the possibility of localized moments. The inset of Fig. 1 displays γ as a function of the field H applied initially along an in-plane direction. A pronounced torque tilted the sample and calorimeter to align the c-axis along H , moving the metamagnetic transition to higher fields. However, one can still clearly see that γ increases by nearly 50 % at the transition indicating the recovery of entropy, i.e., suppression of ordering.

Figure 2 (a) shows the inter-plane resistivity ρ_{zz} for a $\text{Sr}_4\text{Ru}_3\text{O}_{10}$ single crystal at $T \simeq 0.6$ K as a function of H and for several angles θ between H and the inter-plane c-axis. Notice the oscillations in ρ_{zz} , i.e., Shubnikov de Haas (SdH) effect as well as the marked negative magne-

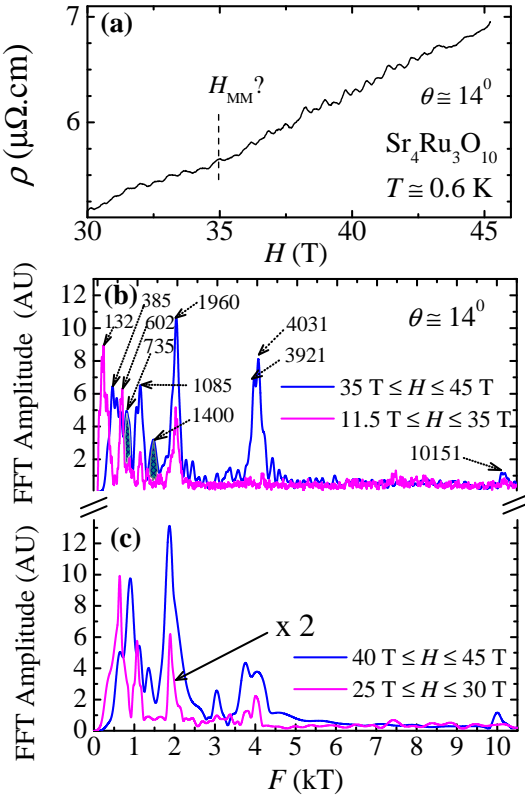


FIG. 3: (a) The in-plane resistivity ρ for a $\text{Sr}_4\text{Ru}_3\text{O}_{10}$ single crystal as a function of H at $T \simeq 0.6$ K and for $\theta = (14 \pm 2)^\circ$ between H and the inter-plane c-axis. The metamagnetic transition does not lead to a clear distinctive feature in ρ . (b) The FFT spectrum of the SdH signal shown for two field ranges, i.e., above (blue line) and below (magenta line) 35 T. (c) The FFT spectrum of the SdH signal shown for two limited field ranges, from 25 to 30 T (in magenta) and from 40 to 45 T (in blue).

toresistivity emerging from the metamagnetic transition. While Fig. 2 (b) displays both ρ_{zz} and its derivative respect to field for an angle $\theta = (17 \pm 2)^\circ$ as a function of H . The oscillatory pattern is clearly affected by the transition, what is confirmed by the FFT spectrum of the Shubnikov-de Haas signal shown in Fig. 2 (c). The peaks observed in the FFT spectrum taken in a range of fields below the transition or $H \leq 34$ T, are clearly displaced to higher frequencies and show additional structures when the FFT is taken in the range $H \geq 34$ T. This indicates that the geometry of these small Fermi surface sheets is affected by the transition.

A more thorough investigation of the effect of the transition on the Fermi surface is given by measurements of the in-plane magnetoresistivity $\rho(H)$ in the highest quality single crystals of $\text{Sr}_4\text{Ru}_3\text{O}_{10}$ currently available, as shown for $\theta = (14 \pm 2)^\circ$ and $T \simeq 0.6$ K in Fig. 3 (a). For reasons that are not clear at the moment, the metamagnetic transition leaves no distinct signature in $\rho(H)$, sug-

gesting perhaps that it involves mainly orbitals oriented along the inter-plane direction such as d_{yz} and d_{zx} . The corresponding Shubnikov-de Haas signal, used in the following Fourier analysis, is defined as $(\sigma - \sigma_b)/\sigma_b$ where $\sigma = 1/\rho$ and σ_b is the inverse of the background resistivity. From our previous angular study of ρ_{zz} in Fig. 2 (a), one expects the metamagnetic transition to happen in the neighborhood of 35 T. Thus in Fig. 3 (b) we display the FFT spectrum of the SdH signal for two ranges of magnetic field, i.e., above (blue line) and below (magenta line) 35 T. The overall spectral weight for frequencies F below 2 kT is rather different between both traces indicating again that H affects mainly the smaller Fermi surface sheets. Since these spectra include a range in H^{-1} where the geometry of parts of the Fermi surface could be poorly defined due to the transition, we show in Fig. 3 (c) both spectra in a different field range, from 25 to 30 T or clearly below the metamagnetic transition (in magenta), and from 40 to 45 T where its geometry is closer to being stable (in blue). The spectra are similar to those in Fig. 3 (b), larger frequencies such as the one close to ~ 2 kT and those around 4 kT, remain unaffected by the transition. However the spectral weight below 2 kT is shifted towards higher frequencies, with an additional peak emerging at ~ 3 kT. The situation here is somewhat similar to that reported in the bi-layered compound $\text{Sr}_3\text{Ru}_2\text{O}_7$ where the FFT spectrum reveals additional structure and small shifts in the frequency of the main peaks across its metamagnetic transition and which are claimed to result from the spin-splitting of the Fermi surface [18].

In Figure 4 (a) we plot the effective mass μ , in units of free electron mass, associated with the peak observed at $F = 1.9$ kT and as a function of H . Here we measured ρ at different temperatures and extracted the corresponding FFT spectrum within a narrow window in $H^{-1} \sim (5T)^{-1}$. The evolution of the amplitude of a given peak in frequency as a function of temperature was fitted to the usual Lifshitz-Kosevich expression $x/\sinh x$ to extract μ . Notice how the value of μ spikes at 36 T, a behavior quite similar to that seen in $\text{Sr}_3\text{Ru}_2\text{O}_7$ and which in this case is perhaps produced by the fluctuations emerging from the metamagnetic quantum-critical end point [18]. Although a metamagnetic quantum-critical end point in the context of itinerant metamagnetism has also been predicted for $\text{Sr}_4\text{Ru}_3\text{O}_{10}$ [2], our attempts to detect for example, an anomalous temperature dependence in the in-plane resistivity have so far yield no indication in its favor. Perhaps, as in the case of $\text{Sr}_3\text{Ru}_2\text{O}_7$ the quantum critical behavior will only emerge when the external field is precisely aligned along the inter-plane c-axis what seems to move the metamagnetic transition beyond the reach of the current continuous fields. In any case, the enhancement of effective mass is also consistent with the scenario of a Zeeman-split Fermi surface that crosses a nearby van-Hove singularity as the field

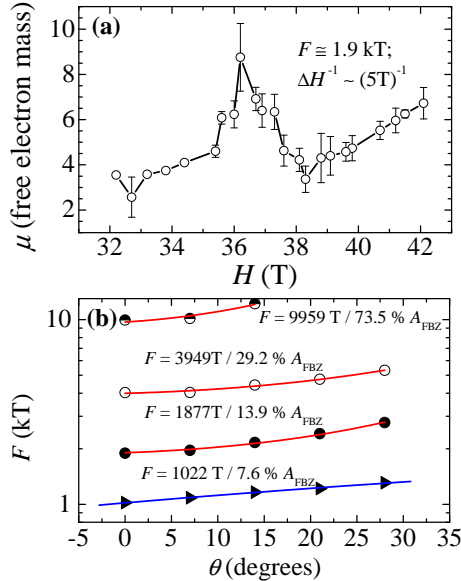


FIG. 4: (a) The magnetic field dependence of the effective mass associated with the FFT peak at $F = 1.9$ kT. The temperature dependence of the FFT spectra was taken within a window in $\Delta(H)^{-1} \simeq (5T)^{-1}$. (b) The angular dependence of the highest frequencies F observed in the FFT spectra. Red lines are fits to the expression $F = F_0 / \cos \theta$ while the blue line is a linear fit. The corresponding cross-sectional areas are also given in percentage of the of the area of the first-Brillouin zone A_{FBZ} .

increases.

Finally, in Fig. 4 (b) we plot the angular dependence of the largest frequencies corresponding to the Fermi surface largest cross-sectional areas. In this compound, as in $\text{Sr}_3\text{Ru}_2\text{O}_7$, the amplitude of the oscillations is quickly damped as θ increases, for unknown reasons. However, we were able to fit (red lines) the angular dependence for the main peaks at 1.9, 3.95, and 9.96 kT to the expression $F = F_0 / \cos \theta$ which clearly indicates their two-dimensional character. Instead, lower frequencies such as the ~ 1 kT display a linear dependence (blue line). The effective masses associated with these orbits averaged over our entire field range are 4.4 ± 0.5 , 5.6 ± 0.3 , 6 ± 1 and 21 ± 6 for the 1.02, 1.9, 3.95 and 9.96 kT frequencies, respectively.

In summary, the overall scenario shown here, i.e., mass enhancement at the metamagnetic transition and the field dependence of the Fermi surface, is quite consistent with an itinerant metamagnetic scenario. What is unique in the present case is to observe this itinerant metamagnetic response within a ferromagnetic state which according to Raman studies, most likely results from localized spins. Otherwise, $\text{Sr}_4\text{Ru}_3\text{O}_{10}$ would represent a quite unique example of itinerant metamagnetic behavior within a itinerant ferromagnetic system. It is interesting to compare the behavior reported here with

the one seen when fields are aligned along an in-plane direction, i.e., domain formation and hysteresis, indicating a strong magnetocrystalline anisotropy [10]. This overall metamagnetic behavior can be explained without invoking the suppression of antiferromagnetic correlations. We owe this complex physical behavior to the multi-band nature of this compound and to its lattice distortions. Orbital-dependent superconductivity in Sr_2RuO_4 [19] and the proposed orbital-selective Mott transition in the $\text{Ca}_{2-x}\text{Sr}_x\text{RuO}_4$ system [14] are other examples of multi-band behavior in ruthenates. Since the Stoner scenario seems too simplistic to explain the ferromagnetism of $\text{Sr}_4\text{Ru}_3\text{O}_{10}$, this compound might provide an unique opportunity for studying the interplay between localized and itinerant states in a all d -electron system.

We acknowledge useful discussions with P. B. Littlewood. The NHMFL is supported by NSF through NSF-DMR-0084173 and the State of Florida. YJJ acknowledges support from the NHMFL-Schuller postdoctoral fellowship program. Z.Q. Mao is a “Cottrell Scholar” and acknowledges support from the Louisiana Board of Regents fund LEQSF(2003-06)-RD-A-26 and pilot fund NSF/LEQSF(2005)-pfund-23 as well as support from the NHMFL’s visiting scientist program. KS also acknowledges the NHMFL’s Visiting Scientist Program. LB was supported by the NHMFL in-house research program.

- [1] E. Stryjewski and N. Giordano, *Adv. Phys.* **26**, 487 (1977).
- [2] B. Binz and M. Sigrist, *Europhys. Lett.* **65**, 816 (2004), and references therein.
- [3] R. S. Perry, *et al.*, *Phys. Rev. Lett.* **86**, 2661 (2001); S. A. Grigera, *et al.*, *Science* **294**, 329 (2001).
- [4] S. A. Grigera, *et al.*, *Science* **306**, 1154 (2004).
- [5] M. Kriener *et al.*, *Phys. Rev. Lett.* **95**, 267403 (2005).
- [6] L. Balicas, *et al.*, *Phys. Rev. Lett.* **95**, 196407 (2005).
- [7] M. K. Crawford *et al.*, *Phys. Rev. B* **65**, 214412 (2002).
- [8] G. Cao *et al.*, *Phys. Rev. B* **68**, 174409 (2003).
- [9] R. Gupta *et al.*, *Phys. Rev. Lett.* **96**, 067004 (2006).
- [10] W. Bao, *et al.*, to be published.
- [11] S. Nakatsuji and Y. Maeno, *Phys. Rev. Lett.* **84**, 2666 (2000); S. Nakatsuji *et al.*, *ibid* **90**, 137202 (2003).
- [12] A. Gukasov *et al.*, *Phys. Rev. Lett.* **89**, 087202 (2002).
- [13] Z. Fang, N. Nagaosa, and K. Terakura, *Phys. Rev. B* **69**, 045116 (2004).
- [14] V. I. Anisimov *et al.*, *Eur. Phys. J. B* **25**, 191 (2002); A. Koga, N. Kawakami, T. M. Rice, and M. Sigrist *Phys. Rev. Lett.* **92**, 216402 (2004) and references therein.
- [15] Z. Q. Mao *et al.*, *Phys. Rev. Lett.* **96**, 077205 (2006).
- [16] M. Zhou *et al.*, *Mater. Res. Bull.* **40**, 942 (2005).
- [17] A. P. Mackenzie *et al.*, *Phys. Rev. Lett.* **76**, 3786 (1996); K. Deguchi, Z. Q. Mao, H. Yaguchi, and Y. Maeno, *ibid* **92**, 047002 (2004).
- [18] R. A. Borzi *et al.*, *Phys. Rev. Lett.* **92**, 216403 (2004).
- [19] D. F. Agterberg, T. M. Rice, and M. Sigrist, *Phys. Rev. Lett.* **78**, 3374 (1997).